



# Design, synthesis, and biological evaluation of 1,3,5-trisubstituted pyrazoles as tyrosine kinase inhibitors

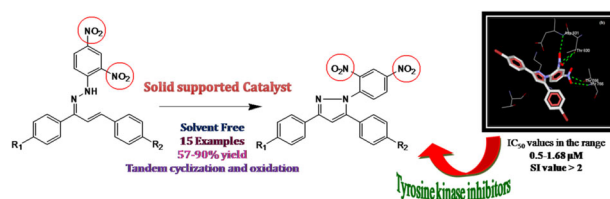
Sinthiya J. Gawandi<sup>1,2</sup> · Vidya G. Desai<sup>1,2</sup> · Sunil G. Shingade<sup>3</sup>

Received: 15 October 2018 / Accepted: 19 December 2018  
© Springer Science+Business Media, LLC, part of Springer Nature 2019

## Abstract

We report herein, silica supported molybdic acid mediated oxidative C–N bond formation for the regioselective synthesis of new 1,3,5-trisubstituted pyrazole derivatives. This transformation furnishes a novel synthetic approach with solvent-free neat heat conditions, which was found to be flexible with wide substrate scope and better efficiency towards rapid synthesis of new 1,3,5-trisubstituted pyrazoles. Selected series of the synthesized derivatives were screened for their liability against carcinogenesis. A molecular docking study of the synthesized derivatives was performed in the active site of the tyrosine kinase enzymes. Based on the molecular docking study specific compounds were screened in vitro for their anticancer activity, which showed potent micro molar activity against human MDA-MB-231 breast cancer line and human leukemia cell line K-562 using 3-(4,5-dimethylthiazol-2-yl)-2, 5-diphenyltetrazolium bromide (MTT) assay. Compound **3i** possesses higher inhibitory activity with  $IC_{50}$   $0.58 \pm 0.02 \mu\text{M}$  against the MDA-MB-231 cell line. Whereas compound **3k** showed higher inhibitory activity with  $IC_{50}$  value  $0.78 \pm 0.03 \mu\text{M}$  against the K-562 cell line. Fluorescence microscopic studies revealed that the compounds showed late apoptotic mode of cell death. These results can lead to further exploitation of tested pyrazole compounds to the highly active drug molecule.

## Graphical Abstract



**Keywords** Hydrazones · Pyrazoles · Solvent-free · Tyrosine kinase · Apoptosis · Anti-proliferative activity

**Supplementary information** The online version of this article (<https://doi.org/10.1007/s00044-018-2282-x>) contains supplementary material, which is available to authorized users.

✉ Vidya G. Desai  
desai\_vidya@gmail.com

- 1 Department of Chemistry, Dnyanprassarak Mandal's College & Research Centre, Assagao, Bardez 403507, India
- 2 Goa University, Taleigao, Panaji 403206, India
- 3 Department of Pharmaceutical Chemistry, PES's Rajaram and Tarabai Bandekar College of Pharmacy, Farmagudi, Ponda, Goa 403401, India

## Introduction

Cancer is one of the major chronic degenerative diseases and a prominent cause of deaths world over. Cancers with high prevalence includes lung, prostate, breast, uterine, and stomach (Ayati et al. 2018). In normal cells, protein kinases play a significant role in regulating the cellular functions of cell metabolism, proliferation, motility, and apoptosis. Inversely, in cancer cells, the expression of different kinases is enhanced thereby, deregulating the functions leading to cell growth and proliferation (Trejo-soto et al. 2018). For instance, breast cancer is a complex and heterogeneous

**Fig. 1** Structures of anticancer drugs containing nitro group

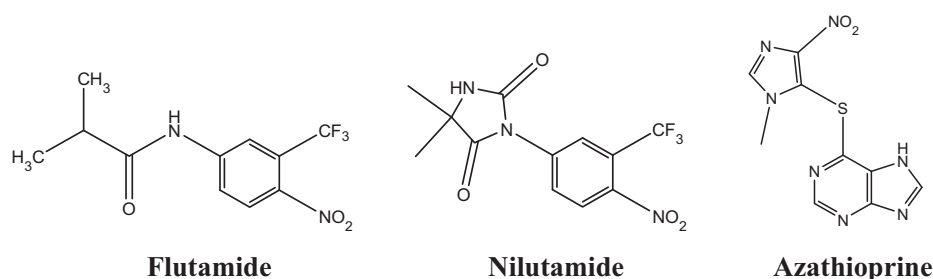
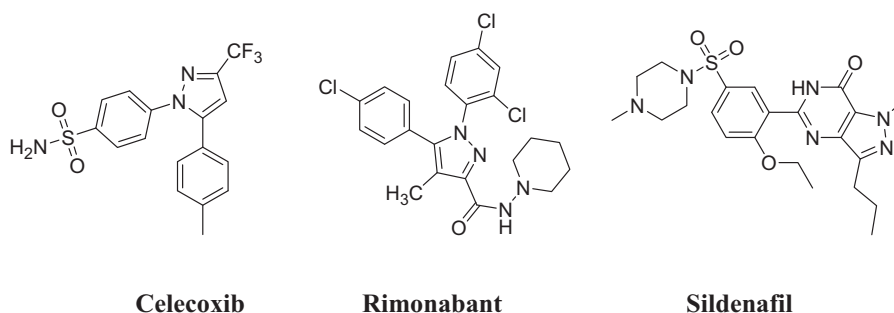


**Fig. 2** Representative structures of clinically important compounds with pyrazole core structures



disease, prevalent in women with around 1.7 million cases diagnosed worldwide every year and the leading cause of death by cancer in women. Existing therapies show detrimental side effects due to their lack of tumor targeting specificity and the emergence of tumor multi-drug resistance (Soudy et al. 2017; Holliday and Speirs 2011).

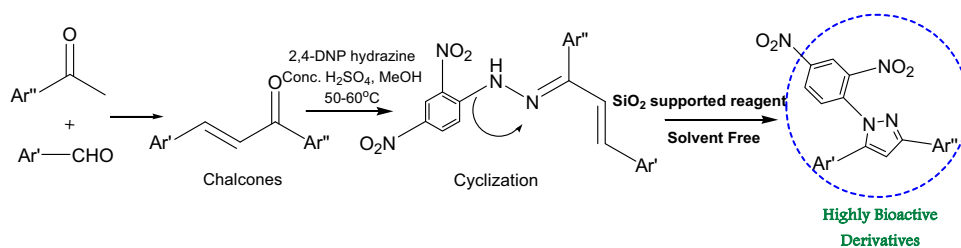
Enzyme inhibition represents an important phenomenon that defines the drug potency and its efficacy. Potency of a drug is measured in the way it can inhibit the activity of enzymes that trigger the cause of disease. Tyrosine kinase, proteasome (Piwowar et al. 2006), DNA topoisomerases (Topcu 2001), histone deacetylases (Mottamal et al. 2015) and so on enzymes have been widely used as a potential target for anticancer agents. Boom of knowledge in molecular sciences, bioinformatics, and proteomics have been an influential factor in the designing of novel enzyme inhibitors. In this aspect, variation in disubstitution pattern plays an important role in the field of drug discovery. Besides the presence of heterocyclic moiety, aryl substitution on a molecule has an influence on the biological activity. Interestingly, nitro group containing aromatic compounds have proved to possess potent activity against different types of cancer diseases. (Fig. 1) (Olender et al. 2018). Thus, with the growing threat of cancer disease, there is an immense need to synthesize a new drug like molecule that can be developed as a better anticancer agent. Tracking on to achieve this goal, we have synthesized a series of new N-aryl hydrazones and converted them into its pyrazole derivatives and evaluated its anticancer activity.

Pyrazoles represent a key structure in heterocyclic chemistry (Abd El-Karim et al. 2015; Kheder et al. 2014; Kumar et al. 2013) and occupies an important place in

medicinal chemistry as it also constitutes the core structure of clinically interesting compounds, such as Celecoxib (Penning et al. 1997; Ahlstrom et al. 2007), Rimonabant, Sildenafil (Mojzych et al. 2015) etc. (Fig. 2). They are also known to possess enzyme inhibiting properties along with diverse biological activities such as, COX inhibitors (Alam et al. 2016), anticancer (Kumar et al. 2013), anti-microbial (Hafez and El-Gazzar 2016), anti-inflammatory (Keche et al. 2012), anti-oxidant (Renuka and Kumar 2013), anti-convulsant, anti-depressant (Abdel-Aziz et al. 2009), anti-pyretic (Malvar et al. 2014), urease inhibitors (Bole et al. 2011), and anti-viral (Tantawy et al. 2012) activity. They also act as cytotoxic agents (Xia et al. 2007), inhibitors of receptors for advanced glycation end products (Han et al. 2014), as dual inhibitors of acetylcholinesterase as well as monoamine oxidase (Kumar et al. 2013).

We previously reported on the synthesis, screening, and preliminary structure activity relationship studies of quinoxalyl chalcone hybrid scaffolds as tyrosine kinase inhibitors (Desai et al. 2017). In our present work, Virtual screening of the pyrazole compounds was carried out targeting tyrosine kinase enzyme for anticancer activity. Very few pyrazole derivatives containing N-2, 4-DNP group have been reported (Deng and Mani 2008; Desai and Naik 2013). Our focus was to achieve synthesis of differently substituted 1-(2, 4-dinitrophenyl)-3,5-diaryl-1H-pyrazoles via oxidative cyclization of stable N-(2,4-dinitrophenyl) hydrazones of chalcones.

The presence of 2,4-dinitrophenyl groups in hydrazones retards the formation of pyrazole. As a result, there are no generalized method for the synthesis of such compounds so, a new ecofriendly protocol for the regioselective synthesis of 1,3,5-trisubstituted pyrazole has been devised (Scheme 1).

**Scheme 1** Design for target compounds

## Material and methods

### Experimental procedure

#### Molecular modeling

**Protein structure preparation** The molecular docking study was performed using Molegro Virtual Docker (MVD-2013, 6.0). The crystal structure of the epidermal growth factor receptor tyrosine kinase domain with 4-anilinoquinazoline inhibitor erlotinib was downloaded from Protein Data Bank PDB ID: 1M17. Molecular docking studies of the synthesized compounds/ligands were performed in order to understand various interactions between the ligand and enzyme active site in detail.

**Molecular docking** The synthesized compounds were built using Chemdraw 11.0. The two-dimensional structures were then converted into energy minimized three-dimensional structures and were saved as MDL Molfile (.mol2). The coordinate files and crystal structures of tyrosine kinase (PDB ID: 1M17) were obtained from the RCSB PDB website. The protein files were prepared by the removal of water molecules, addition of polar hydrogens and removal of other bound ligands. In the present study, the binding sites were selected based on the amino acid residues, which are involved in binding with tyrosine kinase inhibitors as obtained from protein data bank, which would be considered as the probable best accurate regions as they are solved by experimental crystallographic data. The docking protocol was carried out for the synthesized compounds using MVD-2013 (6.0) software using the standard operating procedures (Palkar et al. 2014).

#### Cell culture

Breast cancer cell line MCF-7, leukemia cell line K-562, and human embryonic kidney cell line HEK-293 were purchased from the National Center for Cell sciences (NCCS) Pune. The cell lines were cultured in DMEM medium, i.e., Dulbecco's modified Eagle medium, which were supplemented with 10% heat inactivated fetal calf serum (FBS) and 1% Antibiotic–Antimycotic 100X solution and incubated in CO<sub>2</sub> incubator (Eppendorf, New

Brunswick, Galaxy 170R, Germany) maintained at 37 °C, 5% CO<sub>2</sub> with 95% humidity until the completion of experiments. The absorption spectrum was measured on a JASCO V670 spectrophotometer.

#### Cytotoxicity assay

The breast cancer cell line MDA-MB-231, leukemia cell line K-562, and human non-cancerous cell line HEK-293 were cultured in DMEM medium, which was supplemented with 10% heat inactivated fetal calf serum (FBS) and 1% Antibiotic–Antimycotic 100X solution. The cells were seeded at a density of approximately  $5 \times 10^3$  cells/well in a 96-well flat-bottom micro plate and maintained at 37 °C in 95% humidity and 5% CO<sub>2</sub> for overnight. Different concentration (600, 300, 150, 75, 37.5, 18.75 µg/mL) of test compounds were treated. The cells were incubated for another 72 h. The cells in well were washed twice with phosphate buffer solution, and 20 µL of the MTT staining solution (5 mg/mL in phosphate buffer solution) was added to each well and plate was incubated at 37 °C. After 4 h, 100 µL of dimethyl sulfoxide (DMSO) was added to each well to dissolve the formazan crystals, and absorbance was recorded with a 570 nm using micro plate reader. The IC<sub>50</sub> values were calculated using graph Pad Prism Version 5.1.

#### Double staining (acridine orange-ethidium bromide)

The cells were seeded at a density of approximately  $1 \times 10^4$  cells/well in a 24-well flat-bottom micro plate containing cover slips and maintained at 37 °C in CO<sub>2</sub> incubator for overnight. IC<sub>50</sub> concentration of synthesized compounds was treated at 72 h. After the incubation, cells were washed with PBS and fixed with 4% paraformaldehyde for 30 min. Twenty microliters of dye mixture was incubated for half an hour, examined under fluorescent microscope.

#### DAPI (4',6'-diamine-2'-phenylindole dihydrochloride)

The cells were seeded at a density of approximately  $1 \times 10^5$  cells/well in a 12-well flat-bottom micro plate containing cover slips and maintained at 37 °C in CO<sub>2</sub> incubator for overnight. More than the IC<sub>50</sub> of synthesized compounds was treated at 72 h. After the incubation, cells were washed

with PBS and fixed with 4% paraformaldehyde for 30 min. Twenty microliters of DAPI was incubated for 20 min, examined under fluorescent microscope.

## Chemistry

All commercially available reagents were purchased from SD Fine, LobaChemie, and Avra synthesis and used without further purification. Melting points were determined by open capillary tube method and are uncorrected.  $^1\text{H}$  ( $^{13}\text{C}$ ) nuclear magnetic resonance (NMR) spectra were recorded at Bruker model 400 MHz instrument using  $\text{CDCl}_3$ . The chemical shifts ( $\delta$ ) are expressed in parts per million relative to the residual deuterated solvent signal and coupling constants ( $J$ ) are given in hertz. Proton coupling patterns were illustrated as singlet (s), doublet (d), triplet (t), quartet (q), multiplet (m), and broad (br). IR spectra were recorded on a Shimadzu Fourier transform infrared spectrometer using KBr pellets. High resolution mass spectroscopy data were obtained in electron impact (EI) mode. Intensities are reported as percentages relative to the base peak ( $I = 100\%$ ). Synthesis of new 2, 4-dinitrophenyl hydrazones has been reported by our group (Desai and Gawandi 2016).

### Synthesis of silica chloride

A mixture of silica-gel (5 g) and thionyl chloride (20 mL) was refluxed for 48 h in a round bottomed flask (100 mL) fitted with a condenser and a guard tube containing  $\text{CaCl}_2$ . The resulting white-greyish powder was filtered and dried.

### Synthesis of silica molybdc acid (SMA)

A mixture of silica chloride and sodium molybdate was stirred under refluxing conditions for 3.5 h in n-hexane (5 mL). The reaction mixture was then filtered and washed with distilled water followed by drying at  $120^\circ\text{C}$  in an oven for 6 h. The resulting mixture was then further stirred in 0.1 N HCl solution (40 mL) for 1 h, filtered, washed with distilled water, and dried in an oven at  $120^\circ\text{C}$  for 6 h to obtain the catalyst. Catalyst formation was characterized by XRD analysis. (Ahmed and Siddiqui 2015)

### General procedure for the synthesis of pyrazole derivatives (3a–3o)

Substituted hydrazones (1 mmole) and silica supported molybdc acid (1 mmole) were placed in a conical flask and heated at  $120^\circ\text{C}$ . The progress of the reaction was monitored by TLC. After the completion of the reaction, the product was dissolved in ethyl acetate and filtered to recover the catalyst. The solvent was then evaporated under vacuum and the crude mixture was recrystallized from n-hexane to afford the pure

product. The synthesized compounds were characterized on the basis of IR, NMR and Mass spectroscopic data.

**1-(2,4-dinitrophenyl)-3,5-diphenyl-1H-pyrazole (3a)** Yellow solid, mp:  $142\text{--}144^\circ\text{C}$ ; IR (KBr) ( $\nu_{\text{max}}$ ,  $\text{cm}^{-1}$ ): 3072, 1605, 1538, 1498, 1348 (Desai et al. 2012).

$^1\text{H}$ NMR (400 MHz,  $\text{CDCl}_3$ ) ( $\delta$ , ppm): 8.72 (d, 1H,  $J = 2.44$ , Ar–H), 8.33–8.35 (dd, 1H,  $J = 2.52$ ,  $J = 8.4$ , Ar–H), 7.84 (d, 1H,  $J = 8.4$ , Ar–H), 7.25–7.48 (m, 10H, Ar–H), 6.90 (s, 1H, CH);  $^{13}\text{C}$  NMR (75 MHz,  $\text{CDCl}_3$ ) ( $\delta$ , ppm): 154.6, 146, 145.4, 140.9, 139.6, 136.5, 130.3, 129, 128.5, 127, 120.6, 119.3, 105.3; HRMS (Electrospray ionisation time-of-flight,  $[\text{M}]^+$ ): calcd for  $\text{C}_{21}\text{H}_{14}\text{N}_4\text{O}_4$ , 386.361; found 386.354.

**5-(4-chlorophenyl)-1-(2,4-dinitrophenyl)-3-(4-methoxyphenyl)-1H-pyrazole (3b)** Yellow solid, mp:  $166\text{--}170^\circ\text{C}$ ; IR (KBr) ( $\nu_{\text{max}}$ ,  $\text{cm}^{-1}$ ): 3093, 1608, 1537, 1498, 1348, 1215 (Desai et al. 2012).

$^1\text{H}$ NMR (400 MHz,  $\text{CDCl}_3$ ) ( $\delta$ , ppm): 8.73 (d, 1H,  $J = 2.4$ , Ar–H), 8.33–8.35 (dd, 1H,  $J = 2.44$ ,  $J = 8.8$ , Ar–H), 7.75 (d, 2H,  $J = 8.4$ , Ar–H), 7.44 (d, 1H,  $J = 8.8$ , Ar–H), 6.97–7.36 (m, 6H, Ar–H), 6.82 (s, 1H, CH), 3.85 (s, 3H,  $\text{OCH}_3$ );  $^{13}\text{C}$  NMR (75 MHz,  $\text{CDCl}_3$ ) ( $\delta$ , ppm): 162, 153.9, 146.2, 144.4, 140.3, 139.6, 134.6, 133.8, 130.3, 129.4, 128.8, 128.4, 128, 120.6, 119.3, 114.6, 106.3, 55.6; HRMS (ESI-TOF,  $[\text{M}]^+$ ): calcd for  $\text{C}_{22}\text{H}_{15}\text{N}_4\text{O}_5\text{Cl}$ , 450.832; found 450.823.

**3-(4-bromophenyl)-1-(2,4-dinitrophenyl)-5-(4-methoxyphenyl)-1H-pyrazole (3c)** Yellow solid, mp:  $174\text{--}176^\circ\text{C}$ ; IR (KBr) ( $\nu_{\text{max}}$ ,  $\text{cm}^{-1}$ ): 3087, 1605, 1538, 1498, 1343, 1215, 594.

$^1\text{H}$ NMR (400 MHz,  $\text{CDCl}_3$ ) ( $\delta$ , ppm): 8.72 (d, 1H,  $J = 2.4$ , Ar–H), 8.36–8.38 (dd, 1H,  $J = 0.4$ ,  $J = 8.8$ , Ar–H), 7.77 (d, 2H,  $J = 8.4$ , Ar–H), 7.53 (d, 1H,  $J = 8.8$ , Ar–H), 6.97–7.48 (m, 6H, Ar–H), 6.85 (s, 1H, CH), 3.83 (s, 3H);  $^{13}\text{C}$  NMR (75 MHz,  $\text{CDCl}_3$ ) ( $\delta$ , ppm): 160.8, 154.9, 146.2, 145.3, 144.3, 138.3, 133.6, 133, 130.1, 129.6, 129, 127.4, 124.2, 121.3, 114.2, 111.5, 106.5, 55.6; HRMS (ESI-TOF,  $[\text{M}]^+$ ): calcd for  $\text{C}_{22}\text{H}_{15}\text{N}_4\text{O}_5\text{Br}$ , 494.022; found 494.023.

**1-(2,4-dinitrophenyl)-3,5-bis(4-fluorophenyl)-1H-pyrazole (3d)** Yellow solid, mp:  $172\text{--}174^\circ\text{C}$ ; IR (KBr) ( $\nu_{\text{max}}$ ,  $\text{cm}^{-1}$ ): 3090, 1603, 1535, 1496, 1347, 982.

$^1\text{H}$ NMR (400 MHz,  $\text{CDCl}_3$ ) ( $\delta$ , ppm): 8.75 (d, 1H,  $J = 2.4$ , Ar–H), 8.31–8.33 (dd, 1H,  $J = 2.8$ ,  $J = 8.8$ , Ar–H), 7.87 (d, 2H,  $J = 8.0$ , Ar–H), 7.56 (d, 1H,  $J = 8.8$ , Ar–H), 7.02–7.42 (m, 6H, Ar–H), 6.82 (s, 1H, CH);  $^{13}\text{C}$  NMR (75 MHz,  $\text{CDCl}_3$ ) ( $\delta$ , ppm): 162.1, 158.6, 146.4, 144.6, 139.6, 132.1, 130.1, 128.4, 128., 120.2, 119.3, 116, 106.2; HRMS (ESI-TOF,  $[\text{M}]^+$ ): calcd for  $\text{C}_{21}\text{H}_{12}\text{F}_2\text{N}_4\text{O}_4$ , 422.082; found 422.084

**3,5-bis(4-chlorophenyl)-1-(2,4-dinitrophenyl)-1H-pyrazole**

**(3e):** Yellow solid, mp. 200–206 °C; IR (KBr) ( $\nu_{\max}$ ,  $\text{cm}^{-1}$ ): 3075, 1602, 1532, 1499, 1344, 620

$^1\text{H}$ NMR (400 MHz,  $\text{CDCl}_3$ ) ( $\delta$ , ppm): 8.78 (d, 1H,  $J = 2.4$ , Ar-H), 8.39–8.41 (dd, 1H,  $J = 2.8$ ,  $J = 8.8$ , Ar-H), 7.69 (d, 2H,  $J = 8.4$ , Ar-H), 7.55 (d, 1H,  $J = 8.8$ , Ar-H), 7.10–7.47 (m, 6H, Ar-H), 6.89 (s, 1H, CH);  $^{13}\text{C}$  NMR (75 MHz,  $\text{CDCl}_3$ ) ( $\delta$ , ppm): 153.6, 146.4, 145.3, 144.6, 137.4, 135.2, 132.4, 129.6, 128.2, 123.1, 121.1, 106.5; HRMS (ESI-TOF,  $[\text{M}]^+$ ): calcd for  $\text{C}_{21}\text{H}_{12}\text{Cl}_2\text{N}_4\text{O}_4$ , 454.023; found 454.021

**5-(4-chlorophenyl)-1-(2,4-dinitrophenyl)-3-(4-fluorophenyl)-1H-pyrazole (3f)** Yellow solid, mp. 178–182 °C; IR (KBr) ( $\nu_{\max}$ ,  $\text{cm}^{-1}$ ): 3085, 1608, 1536, 1497, 1348, 989, 614.

$^1\text{H}$ NMR (400 MHz,  $\text{CDCl}_3$ ) ( $\delta$ , ppm): 8.79 (d, 1H,  $J = 2.4$ , Ar-H), 8.36–8.38 (dd, 1H,  $J = 2.42$ ,  $J = 8.8$ , Ar-H), 7.77 (d, 2H,  $J = 8.72$ , Ar-H), 7.57 (d, 1H,  $J = 8.8$ , Ar-H), 6.98–7.42 (m, 6H, Ar-H), 6.83 (s, 1H, CH);  $^{13}\text{C}$  NMR (75 MHz,  $\text{CDCl}_3$ ) ( $\delta$ , ppm): 162.4, 153.6, 146.6, 145.3, 144.5, 139.6, 135.3, 133.1, 132, 130.4, 129.4, 128.6, 128.4, 126.7, 120.6, 114.3, 106.5; HRMS (ESI-TOF,  $[\text{M}]^+$ ): calcd for  $\text{C}_{21}\text{H}_{12}\text{N}_4\text{O}_4\text{ClF}$ , 438.053; found 438.054.

**1-(2,4-dinitrophenyl)-5-(4-methylphenyl)-3-phenyl-1H-pyrazole (3g)** Yellow solid, mp. 154–158 °C; IR (KBr) ( $\nu_{\max}$ ,  $\text{cm}^{-1}$ ): 3087, 1603, 1536, 1496, 1350.

$^1\text{H}$ NMR (400 MHz,  $\text{CDCl}_3$ ) ( $\delta$ , ppm): 8.73 (d, 1H,  $J = 2.4$ , Ar-H), 8.35–8.37 (dd, 1H,  $J = 2.4$ ,  $J = 8.8$ , Ar-H), 7.84 (d, 2H,  $J = 8.4$ , Ar-H), 7.49 (d, 1H,  $J = 8.8$ , Ar-H), 7.05–7.43 (m, 7H, Ar-H), 6.83 (s, 1H, CH), 2.38 (s, 3H,  $\text{CH}_3$ );  $^{13}\text{C}$  NMR (75 MHz,  $\text{CDCl}_3$ ) ( $\delta$ , ppm): 154.6, 146, 145.8, 145.2, 139.6, 138.2, 131.8, 129.8, 129.6, 128.9, 128.8, 128.5, 127, 126, 125.7, 120.9, 106.3, 21.37; HRMS (ESI-TOF,  $[\text{M}]^+$ ): calcd for  $\text{C}_{22}\text{H}_{16}\text{N}_4\text{O}_4$ , 400.117; found 400.119.

**3-(4-bromophenyl)-5-(4-chlorophenyl)-1-(2,4-dinitrophenyl)-1H-pyrazole (3h)** Yellow solid, mp. 138–142 °C; IR (KBr) ( $\nu_{\max}$ ,  $\text{cm}^{-1}$ ): 3085, 1608, 1539, 1495, 1348, 742, 552 (Desai et al. 2012).

$^1\text{H}$ NMR (400 MHz,  $\text{CDCl}_3$ ) ( $\delta$ , ppm): 8.79 (d, 1H,  $J = 2.4$ , Ar-H), 8.36–8.38 (dd, 1H,  $J = 2.44$ ,  $J = 8.8$ , Ar-H), 7.69 (d, 2H,  $J = 8.4$ , Ar-H), 7.45 (d, 1H,  $J = 8.8$ , Ar-H), 7.10–7.58 (m, 6H, Ar-H), 6.89 (s, 1H, CH);  $^{13}\text{C}$  NMR (75 MHz,  $\text{CDCl}_3$ ) ( $\delta$ , ppm): 153.6, 146.2, 145.3, 144.9, 137.7, 134.9, 132.5, 130.1, 129.6, 129.4, 129, 128.6, 127.3, 127.2, 124.1, 121.1, 106.6; HRMS (ESI-TOF,  $[\text{M}]^+$ ): calcd for  $\text{C}_{21}\text{H}_{12}\text{N}_4\text{O}_4\text{ClBr}$ , 497.972; found 497.98.

**1-(2,4-dinitrophenyl)-3-(4-fluorophenyl)-5-(4-methoxyphenyl)-1H-pyrazole (3i)** Yellow solid, mp. 142–144 °C; IR (KBr) ( $\nu_{\max}$ ,  $\text{cm}^{-1}$ ): 3093, 1608, 1537, 1498, 1348, 1215.

$^1\text{H}$ NMR (400 MHz,  $\text{CDCl}_3$ ) ( $\delta$ , ppm): 8.75 (d, 1H,  $J = 2.4$ , Ar-H), 8.35–8.38 (dd, 1H,  $J = 2.4$ ,  $J = 8.8$ , Ar-H), 7.81 (d, 2H,  $J = 7.2$ , Ar-H), 7.48 (d, 1H,  $J = 8.8$ , Ar-H), 6.88–7.26 (m, 6H, Ar-H), 6.79 (s, 1H, CH), 3.83 (s, 3H,  $\text{OCH}_3$ );  $^{13}\text{C}$  NMR (75 MHz,  $\text{CDCl}_3$ ) ( $\delta$ , ppm): 164.2, 160.2, 154.3, 145.9, 145.2, 144.6, 138.1, 130.1, 129.5, 127.8, 127.1, 120.9, 120.6, 115.9, 115.6, 114.6, 105.9, 55.8; HRMS (ESI-TOF,  $[\text{M}]^+$ ): calcd for  $\text{C}_{22}\text{H}_{15}\text{N}_4\text{O}_5\text{F}$ , 434.103; found 434.101.

**1-(2,4-dinitrophenyl)-3,5-bis(4-methoxyphenyl)-1H-pyrazole (3j)** Yellow solid, mp. 168–170 °C; IR (KBr) ( $\nu_{\max}$ ,  $\text{cm}^{-1}$ ): 3105, 1605, 1538, 1505, 1215 (Desai et al. 2012).

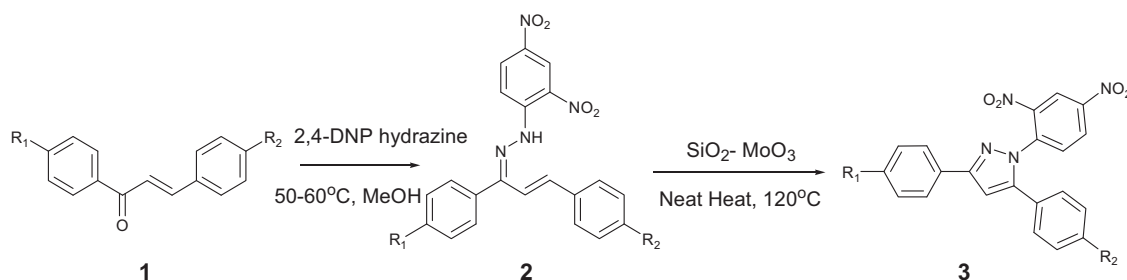
$^1\text{H}$ NMR (400 MHz,  $\text{CDCl}_3$ ) ( $\delta$ , ppm): 8.73 (d, 1H,  $J = 2.4$ , Ar-H), 8.32–8.34 (dd, 1H,  $J = 2.44$ ,  $J = 8.8$ , Ar-H), 7.78 (d, 2H,  $J = 8.6$ , Ar-H), 7.50 (d, 1H,  $J = 8.8$ , Ar-H), 6.91–7.28 (m, 6H, Ar-H), 6.79 (s, 1H, CH), 3.87 (s, 3H,  $\text{OCH}_3$ ), 3.85 (s, 3H,  $\text{OCH}_3$ );  $^{13}\text{C}$  NMR (75 MHz,  $\text{CDCl}_3$ ) ( $\delta$ , ppm): 160.2, 154.5, 146, 145.2, 144.6, 137.8, 132.4, 130.1, 129.5, 127.4, 120.4, 114.2, 56.4; HRMS (ESI-TOF,  $[\text{M}]^+$ ): calcd for  $\text{C}_{23}\text{H}_{18}\text{N}_4\text{O}_6$ , 446.122; found 446.126.

**3,5-bis(4-bromophenyl)-1-(2,4-dinitrophenyl)-1H-pyrazole (3k)** Yellow solid, mp. 192–196 °C; IR (KBr) ( $\nu_{\max}$ ,  $\text{cm}^{-1}$ ): 3098, 1602, 1532, 1496, 1348, 572;  $^1\text{H}$ NMR (400 MHz,  $\text{CDCl}_3$ ) ( $\delta$ , ppm): 8.75 (d, 1H,  $J = 2.4$ , Ar-H), 8.31–8.33 (dd, 1H,  $J = 2.8$ ,  $J = 8.8$ , Ar-H), 7.87 (d, 2H,  $J = 8.4$ , Ar-H), 7.53 (d, 1H,  $J = 8.8$ , Ar-H), 7.03–7.45 (m, 6H, Ar-H), 6.85 (s, 1H, CH);  $^{13}\text{C}$  NMR (75 MHz,  $\text{CDCl}_3$ ) ( $\delta$ , ppm): 154.6, 146.4, 145.3, 137.6, 132.4, 130.3, 128.6, 128.2, 123.1, 120.2, 119.3, 116.1, 106.2; HRMS (ESI-TOF,  $[\text{M}]^+$ ): calcd for  $\text{C}_{21}\text{H}_{12}\text{Br}_2\text{N}_4\text{O}_4$ , 541.922; found 541.920.

**3-(4-bromophenyl)-1-(2,4-dinitrophenyl)-5-(4-methylphenyl)-1H-pyrazole (3l)** Yellow solid, mp. 182–185 °C; IR (KBr) ( $\nu_{\max}$ ,  $\text{cm}^{-1}$ ): 3087, 1605, 1538, 1498, 1343, 594.

$^1\text{H}$ NMR (400 MHz,  $\text{CDCl}_3$ ) ( $\delta$ , ppm): 8.72 (d, 1H,  $J = 2.4$ , Ar-H), 8.34–8.37 (dd, 1H,  $J = 2.4$ ,  $J = 8.4$ , Ar-H), 7.81 (d, 2H,  $J = 8.0$ , Ar-H), 7.55 (d, 1H,  $J = 8.4$ , Ar-H), 7.17–7.50 (m, 6H, Ar-H), 6.85 (s, 1H, CH), 2.38 (s, 3H);  $^{13}\text{C}$  NMR (75 MHz,  $\text{CDCl}_3$ ) ( $\delta$ , ppm): 154.6, 146.2, 145.8, 145.18, 139.7, 138.3, 131.8, 129.8, 129.6, 128.9, 128.4, 127., 125.7, 123.5, 120.9, 106.4, 21.4; HRMS (ESI-TOF,  $[\text{M}]^+$ ): calcd for  $\text{C}_{22}\text{H}_{15}\text{N}_4\text{O}_5\text{Br}$ , 494.022; found 494.023.

**1-(2,4-dinitrophenyl)-3-(4-methoxyphenyl)-5-(4-methylphenyl)-1H-pyrazole (3m)** Yellow solid, mp. 142–148 °C; IR (KBr) ( $\nu_{\max}$ ,  $\text{cm}^{-1}$ ): 3097, 1603, 1542, 1445, 1349, 1217.  $^1\text{H}$ NMR (400 MHz,  $\text{CDCl}_3$ ) ( $\delta$ , ppm): 8.72 (d, 1H,  $J = 2.4$ , Ar-H), 8.33–8.36 (dd, 1H,  $J = 2.8$ ,  $J = 8.8$ , Ar-H), 7.77 (d, 2H,  $J = 8.4$ , Ar-H), 7.46 (d, 1H,  $J = 8.8$ , Ar-H), 6.94–7.26. (m, 6H, Ar-H), 6.80 (s, 1H, CH), 3.85 (s, 3H,  $\text{OCH}_3$ ), 2.38 (s, 3H,  $\text{CH}_3$ );  $^{13}\text{C}$  NMR (75 MHz,  $\text{CDCl}_3$ ) ( $\delta$ ,



**Scheme 2** Synthesis of 1,3,5-trisubstituted pyrazoles

ppm): 160.8, 154.9, 146.2, 145.3, 144.3, 138.3, 133.6, 133, 130.1, 129.6, 129, 127.4, 124.2, 121.3, 114.2, 111.5, 106.5, 55.6, 21.3; HRMS (ESI-TOF,  $[M]^+$ ): calcd for  $C_{23}H_{18}N_4O_5$ , 430.128; found 430.129.

**1-(2,4-dinitrophenyl)-5-(4-fluorophenyl)-3-(4-hydroxyphenyl)-1H-pyrazole (3n)** Yellow solid, mp. 206–208 °C; IR (KBr) ( $\nu_{\max}$ ,  $cm^{-1}$ ): 3596, 3076, 1601, 1532, 1489, 1342, 980.

$^1H$ NMR (400 MHz,  $CDCl_3$ ) ( $\delta$ , ppm): 8.73 (d, 1H,  $J = 2.4$ , Ar-H), 8.36–8.39 (dd, 1H,  $J = 2.4$ ,  $J = 8.8$ , Ar-H), 7.75 (d, 2H,  $J = 6.4$ , Ar-H), 7.46 (d, 1H,  $J = 8.8$ , Ar-H) 6.88–7.26 (m, 6H, Ar-H), 6.80 (s, 1H, CH);  $^{13}C$  NMR (75 MHz,  $CDCl_3$ ) ( $\delta$ , ppm): 160.8, 154.9, 152.4, 146.2, 145.3, 144.3, 138.3, 133.6, 132.2, 130.1, 129.6, 128.4, 127.2, 120.9, 116.2, 116.5, 106.5; HRMS (ESI-TOF,  $[M]^+$ ): calcd for  $C_{21}H_{13}N_4O_5F$ , 420.087; found 420.080.

**1-(2,4-dinitrophenyl)-5-(4-nitrophenyl)-3-phenyl-1H-pyrazole (3o)** Yellow solid, mp. 224–226 °C. IR (KBr) ( $\nu_{\max}$ ,  $cm^{-1}$ ): 3089, 1603, 1540, 1484, 1350.

$^1H$ NMR (400 MHz,  $CDCl_3$ ) ( $\delta$ , ppm): 8.79 (d, 1H,  $J = 2.4$ , Ar-H), 8.41–8.44 (dd, 1H,  $J = 2.4$ ,  $J = 8.6$ , Ar-H), 8.25 (d, 2H,  $J = 7.2$ , Ar-H), 7.84 (d, 1H,  $J = 8.6$ , Ar-H), 7.26–7.51 (m, 7H, Ar-H), 7.03 (s, 1H, CH);  $^{13}C$  NMR (75 MHz,  $CDCl_3$ ) ( $\delta$ , ppm): 154.6, 148.3, 146.4, 145.8, 144.4, 139.6, 138.4, 131.8, 129.8, 129.4, 128.9, 128.8, 128.5, 127.5, 124.3, 120.9, 106.3; HRMS (ESI-TOF,  $[M]^+$ ): calcd for  $C_{21}H_{13}N_5O_6$ , 431.086; found 431.102.

## Results and discussion

Our preliminary investigations were focused on the development of an ecofriendly reaction conditions for effecting oxidative cyclization. To achieve this, screening of various catalysts and solvents has been carried out. The results revealed that the most suitable reagent for this transformation was  $SiO_2$ -molybdic acid, which was then followed by further optimization of reaction conditions. We investigated the effect of the catalyst loading and effect of temperature

**Table 1** List of 1,3,5-trisubstituted pyrazole derivatives

Compounds	R <sub>1</sub>	R <sub>2</sub>	Time in hours	% Yield
<b>3a</b>	H	H	4	66
<b>3b</b>	OMe	Cl	3	77
<b>3c</b>	Br	OMe	4	73
<b>3d</b>	F	F	2.5	78
<b>3e</b>	Cl	Cl	3	88
<b>3f</b>	F	Cl	3.5	84
<b>3g</b>	H	CH <sub>3</sub>	4	81
<b>3h</b>	Br	Cl	1.5	66
<b>3i</b>	F	OMe	1.5	60
<b>3j</b>	OMe	OMe	3.5	57
<b>3k</b>	Br	Br	2.5	79
<b>3l</b>	Br	CH <sub>3</sub>	1.5	60
<b>3m</b>	OMe	CH <sub>3</sub>	2	86
<b>3n</b>	OH	F	2.5	79
<b>3o</b>	NO <sub>2</sub>	H	3	76

on the model reaction. It was observed that, catalyst not in mol%, but in equimolar amount gave good yield of the cyclized product at 120 °C.

Once the optimized conditions had been developed, we examined the substrate scope and generality of the desired oxidative cyclization reaction. A wide range of newly synthesized substituted 2,4-dinitrophenyl hydrazone derivatives were used for the synthesis of 1,3,5-trisubstituted pyrazoles (**3a–3o**) (Scheme 2) (Desai and Gawandi 2016). As shown in Table 1, respective hydrazones and equivalent amount of catalyst were heated at 120 °C. After completion, the reaction mixture was washed with ethyl acetate and catalyst was filtered off. Solvent was removed on vacuum and the crude product was recrystallized using n-hexane. It is also worth noting that the purification procedure for the synthesized compounds required only recrystallization instead of tedious and prolonged column chromatographic technique. In order to check the effectiveness of silica molybdic acid, its recycling was performed and was inferred that it can be used over five cycles of reaction without much loss in activity.

**Table 2** Molegro docking score for pyrazole derivatives (**3a–3o**) for anticancer activity

Code	MolDock score (Kcal/mol)	Rerank score (Kcal/mol)	E-inter (protein-ligand)	HBond		Heavy atoms count	Docking score (Kcal/mol)
				No.	Kcal/mol		
<b>3a</b>	-136.051	-90.2738	-132.572	3	-3.46377	29	-139.951
<b>3b</b>	-144.917	-98.7802	-142.843	3	-4.27694	32	-148.045
<b>3c</b>	-149.881	-101.725	-143.373	4	-6.81212	32	-151.798
<b>3d</b>	-148.618	-96.6649	-141.006	5	-6.88374	31	-150.723
<b>3e</b>	-144.812	-82.0598	-137.168	3	-4.70957	31	-144.842
<b>3f</b>	-145.328	-83.7235	-137.104	3	-4.71109	31	-145.484
<b>3g</b>	-137.869	-31.2169	-135.422	0	0	30	-135.477
<b>3h</b>	-138.83	-78.3858	-140.427	7	-10.4638	31	-146.55
<b>3i</b>	-152.306	-90.566	-144.484	3	-4.57163	32	-152.181
<b>3j</b>	-148.609	-98.5868	-141.134	1	-2.05601	33	-148.955
<b>3k</b>	-161.223	-108.857	-152.841	1	-1.90323	31	-159.651
<b>3l</b>	-144.452	-83.159	-136.202	3	-4.71239	31	-144.564
<b>3m</b>	-128.389	-33.1833	-124.899	6	-9.61717	32	-141.594
<b>3n</b>	-141.867	-47.023	-134.386	6	-9.80866	31	-152.178
<b>3o</b>	-158.518	-105.681	-153.638	7	-9.10727	32	-160.755

Under these experimental conditions, cyclization took place better in the presence of electron withdrawing groups on aromatic ring. Compound **3e** with electron withdrawing chloro group at 4 positions of 3 and 5 substituted aromatic ring gave excellent yield in 88% in comparison to compound **3a** with no substituents in aromatic ring, obtained in 66% yield. On the other side, compound **3j** with electron donating methoxy substituent was obtained in 57% yield. Thus, the nature of substituent alters the reactivity of the substrate towards cyclization.

All the synthesized compounds were characterized by IR,  $^1\text{H}$  NMR,  $^{13}\text{C}$  NMR spectroscopy, and mass spectroscopy. The IR spectra of the title products **3a–3o** exhibited characteristic absorption bands at 3095 to 3070  $\text{cm}^{-1}$  indicating the C–H bond of the pyrazole ring. Also disappearance of absorption bands in the region of frequency at 3300  $\text{cm}^{-1}$  pertaining to N–H bond confirms the conversion of hydrazone derivatives to pyrazole. Absorption bands at 1600 to 1610  $\text{cm}^{-1}$  could be attributed to the presence of C=N bond. Characteristic absorption peak at 1540 to 1550  $\text{cm}^{-1}$  corresponds to the ( $-\text{NO}_2$ ) nitro group attached to the carbon atom.  $^1\text{H}$  NMR analysis further confirms the pyrazole structure. The main distinctive peak in the spectra of all the target compounds is the appearance of the singlet  $\delta\text{H}$  at 6.5 to 7.5 ppm signifying the proton attached to C4 of the five membered pyrazole ring. The most deshielded proton was observed in case of the aromatic hydrogen present between the two nitro groups as a doublet at  $\delta\text{H}$  8.79–8.72 ppm. All the aromatic protons showed multiplets at  $\delta\text{H}$  7.50 to 7.10 ppm, thereby marking the formation of pyrazole derivatives. Along with this,  $^{13}\text{C}$  NMR spectroscopic study also signifies the pyrazole

formation. Chemical shifts at 154.3, 146.8, 144.4, and 106.2 ppm corresponds to C5=N, C4- $\text{NO}_2$ , C3-N, and C4-H carbon atoms. The exact molecular weight was also characterized and confirmed by HRMS studies. The ultraviolet spectroscopic studies showed absorbance values at 246 nm.

## Anticancer activity

### Virtual screening

The synthesized pyrazole compounds were virtually screened for its anticancer activity using tyrosine kinase as the target enzyme (Table 2). The molecular docking study revealed that the compounds **3i**, **3k**, and **3l** act as a very good inhibitors of tyrosine kinase enzyme. As depicted in Fig. 3 compound **3i** makes two hydrogen bonding interactions at the active site of the enzyme, among them one interaction comes from the oxygen atom of methoxy group present at fourth position of aromatic ring with Gly772 (1.55 Å) and the other interaction from the oxygen atom of nitro group present on the fourth position of another aromatic ring with Cys773 (2 Å).

The nitro group present on the second and fourth position of aromatic rings in compound **3k** makes five hydrogen bonding interactions out of which two are observed between nitrogen and oxygen of nitro group and Thr766 (1.52 and 1.55 Å). The oxygen atoms of nitro group show two interactions with Asp831 (1.55 Å) and Thr830 (1.52 Å) and the nitrogen of nitro group shows one interaction with Thr830 (1.52 Å).

Compound **3l** makes two hydrogen bond interactions, the nitrogen and oxygen atoms of nitro group present on fourth

**Fig. 3** Molecular docking data: The compounds docked in best of its conformation into the binding site of IM17. **a** Binding mode of compound **3i** forming one H bond with Cys773, one H bond with Gly772; **b** binding mode of compound **3k** forming one H bond with Asp831, two H bonds with Thr830, two H bonds with Thr766; **c** binding mode of compound **3l** forming two H bonds with Met76

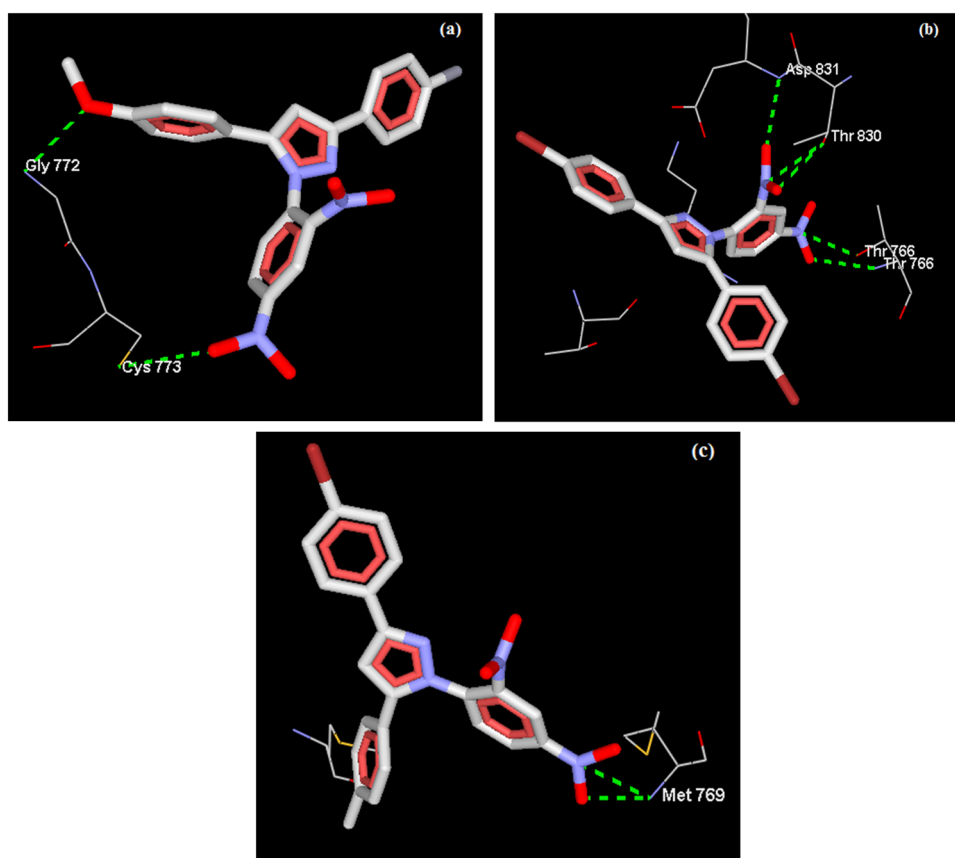


**Table 3** IC<sub>50</sub> values (μM ± S.E.) of compounds **3i**, **3k**, and **3l** against two different cancer cell lines and normal human cell lines

Compounds	MDA-MB-231 <sup>a</sup>	K-562 <sup>b</sup>	HEK-293 <sup>c</sup>	SI <sup>d</sup> -MDA-MB-231	SI K-562
<b>3i</b>	0.93 ± 0.05	1.68 ± 0.08	4.41 ± 0.09	4.70	2.62
<b>3k</b>	0.68 ± 0.04	0.78 ± 0.03	6.02 ± 0.1	8.86	7.72
<b>3l</b>	0.58 ± 0.02	1.22 ± 0.06	39.24 ± 0.12	66.96	32.16
Doxorubicin	0.08 ± 0.01	4.49 ± 1.39	–	–	–
Paclitaxel	0.3 ± 0.02	>100	–	–	–

<sup>a</sup>MDA-MB-231-triple negative breast cancer cell line

<sup>b</sup>K-562- Myelogenous leukemia cell line

<sup>c</sup>HEK-293-human embryonic kidney cells (human non-tumorous cells)

<sup>d</sup>Selective index was calculated as ratio of IC<sub>50</sub> value of non-tumorous cell line to the IC<sub>50</sub> value of cancer cell line. IC<sub>50</sub> values are obtained as the mean ± SD (μM) from three different experiments

position of aromatic ring shows interactions with Met769 (1.55 Å) (Fig 3).

### Biological screening

**Cancer cell inhibitory activities of the selected compounds** On the basis of the enzymatic inhibitory potency against IM17, compounds **3i**, **3k**, and **3l** were selected and evaluated for their anti-proliferative activity against breast cancer cell line MDA-MB-231 (ER-negative) and myelogenous leukemia cell line K-562 using MTT(3-

(4,5-dimethylthiazol-2-yl)-2,5-diphenyltetrazolium bromide) assay method.

All the three selected pyrazole compounds inhibited cell proliferation with IC<sub>50</sub> values in the range of 0.58 to 1.68 μM. As shown in Table 3, the samples showed moderate to good activity comparable to that of standard drugs, especially compound **3l** showed higher anti-proliferation activity with IC<sub>50</sub> = 0.58 ± 0.02 μM against TNBC(triple negative breast cancer) MDA-MB-231 cell lines. Also, compound **3l** exhibited moderate activity with IC<sub>50</sub> value 1.22 ± 0.06 μM against K-562-leukemia cell line.

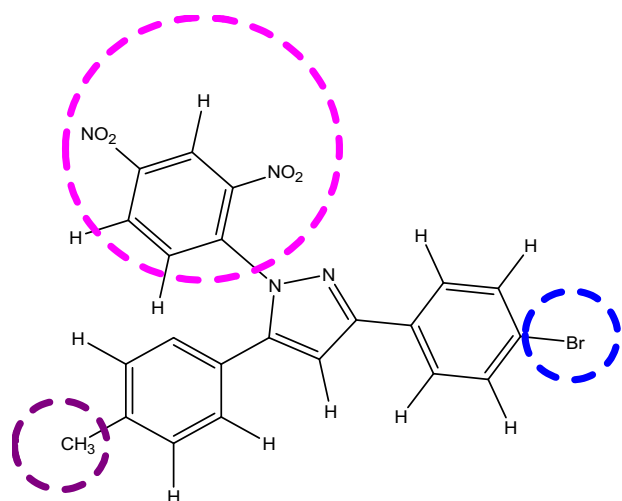


**Fig. 4** Structural features of compound **3i** responsible for anticancer activity

Compounds **3i** and **3k** showed moderate activity with  $IC_{50}$  values  $0.93 \pm 0.05$  and  $0.68 \pm 0.04 \mu\text{M}$  against MDA-MB-231 cell lines. In case of K-562 cell line, compound **3k** displayed higher anti-proliferative activity with  $IC_{50}$  value  $0.78 \pm 0.03 \mu\text{M}$  as compared to the other two screened samples, which was compatible with its docking study.

Accompanying this, the in vitro cytotoxic activity of all the tested compounds was assessed against normal HEK-293 cell lines by MTT colorimetric assay. The cytotoxic results revealed that none of the three evaluated compounds exhibited any significant toxicity effect on normal HEK-293 cells. SI, i.e., selectivity index exposes the differential activity of a pure compound. Compound with a higher SI value is said to be more selective and hence less cytotoxic. On the other side, a compound with SI value  $< 2$  indicates cytotoxicity of the pure compound. As seen in Table 3 all

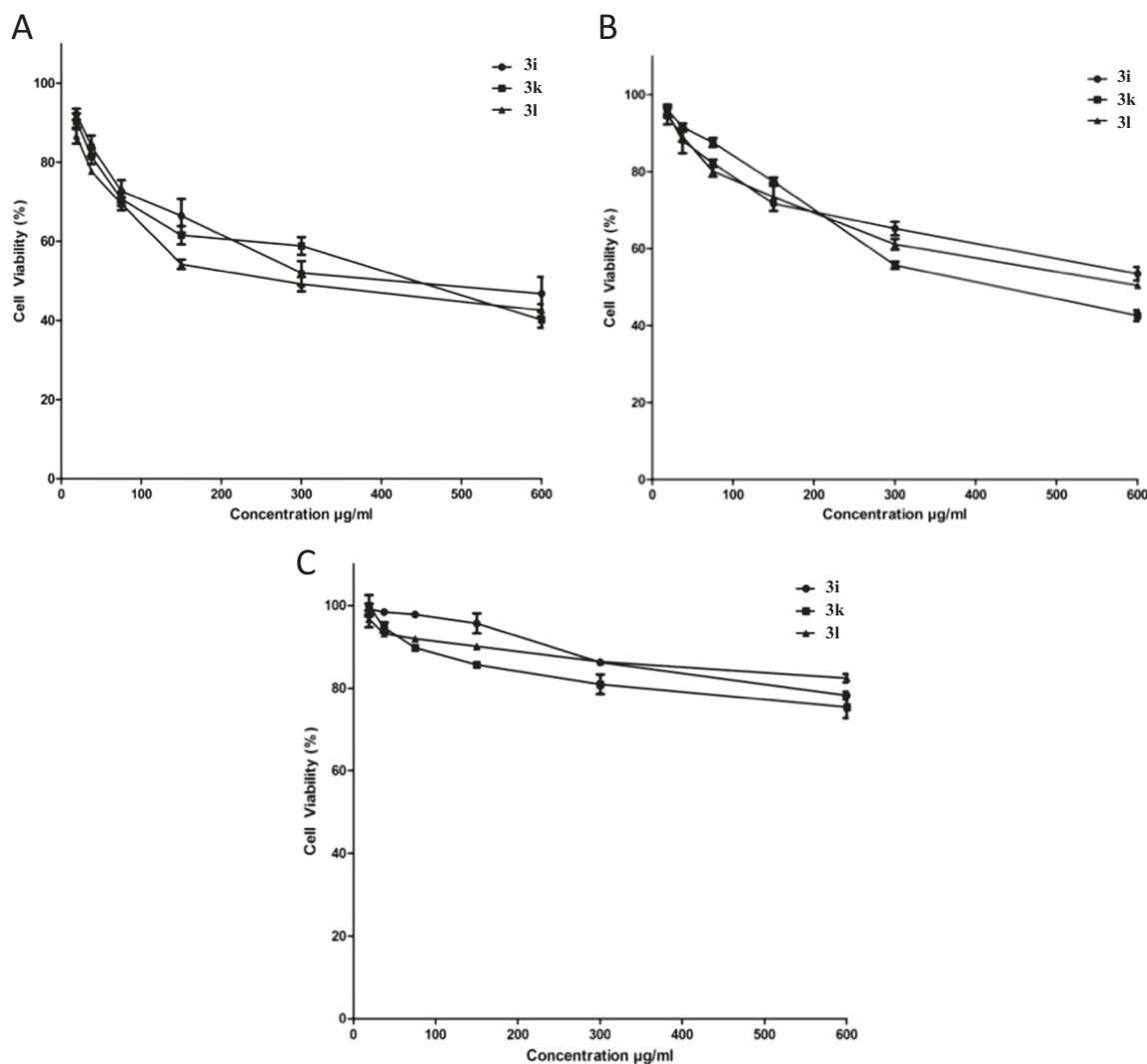
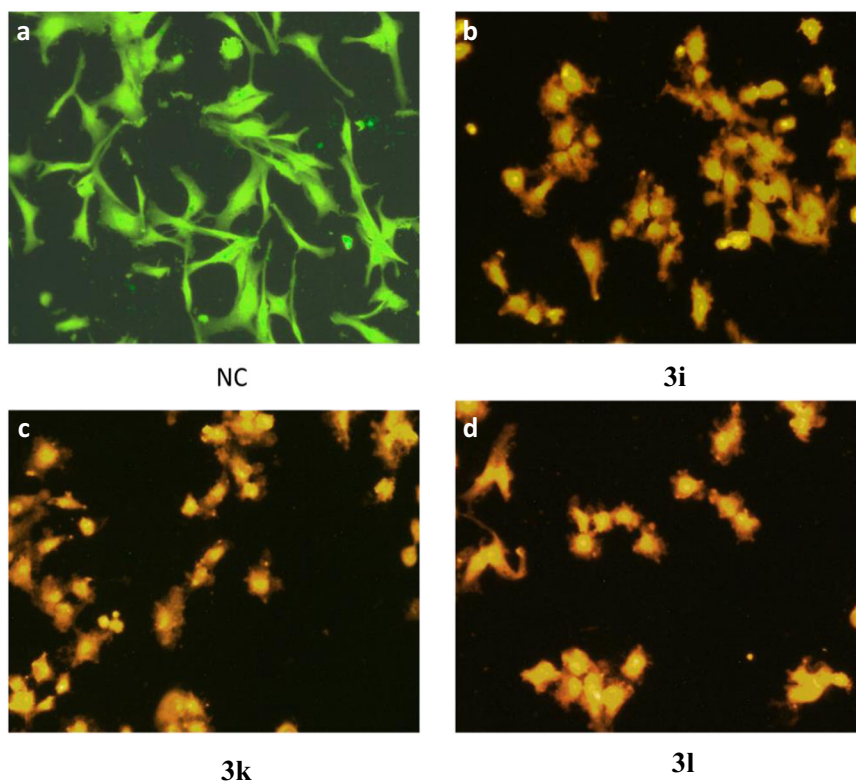


**Fig. 5** Graphical representation of cell viability exhibited by **3i**, **3k**, and **3l** for three different cell lines. **a** For MDA-MB-231 cell line, **b** for K-562 cell line, and **c** HEK-293 (non-tumorous) cell line

**Fig. 6** Fluorescence microscopy images of cells stained with acridine orange/ethidium bromide. **a** Viable untreated cells, **b** cells treated with compound **3i**, **c** cells treated with compound **3k**, **d** cells treated with compound **3l**



the samples were proved to be non toxic on the normal tumor cells (Fig. 4).

As seen in Fig. 5; the effect of pyrazole derivatives on the viability of MDA-MB-231, K-562 human cancer cell lines and HEK-293 was investigated and represented graphically as variation in percentage of viability with respect to time and concentration.

### Cell morphology studies by fluorescence microscopy

Fluorescence microscopy study was used to study how cell death was induced by selected pyrazole compounds **3i**, **3k**, and **3l** in comparison to the standard cis-platin by virtue of acridine orange/ ethidium bromide staining. The fluorescence properties of dyes can help to characterize the mode of cell death, whether early or late apoptosis. Acridine orange is taken up by both viable and apoptotic (dead) cells by emitting green fluorescence. Ethidium bromide will stain only cells with disrupted membrane integrity, i.e., late apoptotic cells and necrotic cells. Staining of acridine orange on live cells showed green fluorescent nuclei, which indicate early apoptosis, while late apoptotic cells have orange to red nuclei with condensed or fragmented chromatin. Necrotic cells have uniform orange to red nuclei with the organized structure. Thus, the results (Fig. 6) demonstrated that the viable cells without treatment of pyrazole compound stained with acridine orange appeared with green fluorescent nucleus Fig. 6a, while late apoptotic cells

showed an orange fluorescence with nuclear membrane bebling Fig. 6b–d thereby signifying the apoptotic mode of cell death.

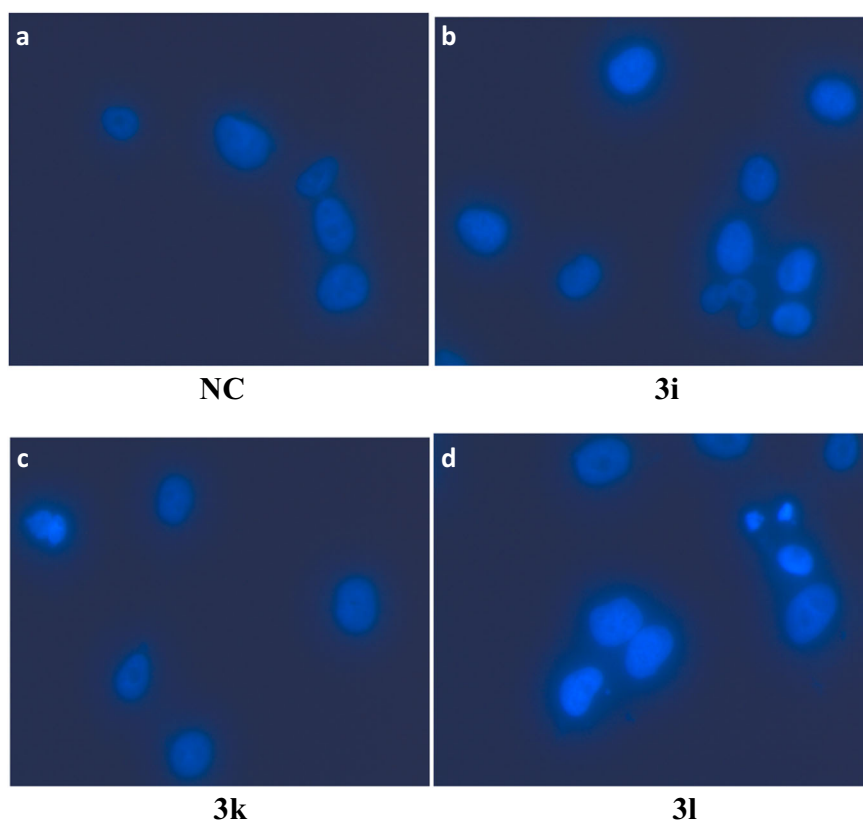
Further, an apoptotic mode of cell death was confirmed by fluorescence microscopy studies using DAPI staining method wherein, the treated and untreated cells were stained with 4',6-diamidino-2'-phenylindole dihydrochloride (DAPI). As shown in Fig. 7 the cell shrinkage, nuclear fragmentation characterizes the apoptotic mode of cell death by cells treated with compound **3i**, **3k**, and **3l** stained with DAPI.

### Conclusion

In conclusion, a novel series of 2,4-dinitrophenyl containing pyrazole derivatives (**3a–3o**) were designed, synthesized, and evaluated as anti-proliferative agents. Keeping in view the significance of presence of electron withdrawing nitro groups, our efforts of achieving oxidative cyclization of N-aryl hydrazones has led to a novel class of bioactive pyrazoles of different substitution patterns in good yields. Recycling of the reagent up to five cycles without any higher loss in catalytic activity and time consumption delivers the efficiency of the green method.

Considering the biological screening results, the pyrazole derivatives showed potent anticancer activity against the MDA-MB-231(ER-negative) human breast cancer cell line

**Fig. 7** Fluorescence microscopy images of cells stained with DAPI, showing **a** viable untreated cells, **b** cells treated with compound **3i**, **c** cells treated with compound **3k**, **d** cells treated with compound **3l**



and K-562 leukemia cell line. It was noticed that the selective compounds **3i**, **3k**, and **3l** demonstrated significant minimum inhibitory activity with  $IC_{50}$  values in the range 0.5–1.68  $\mu$ M against cancer cell lines MDA-MB-231 and K-562. Cytotoxicity against the human embryonic kidney cell line HEK-293 was also evaluated and the selectivity was thus assessed. The evaluated compounds displayed moderate SI values ranging from 2.62 to 32.16. The docking studies revealed that compounds **3i**, **3k**, and **3l** had good tyrosine kinase binding interactions. Further, the mode of cell death was characterized by fluorescence microscopy study, to be late apoptosis, which was also supported by DAPI results.

These results were compatible with the docking studies, which revealed that compounds **3i**, **3k**, and **3l** act as potent inhibitor of tyrosine kinase by virtue of hydrogen bonding interactions with nitro group of the aromatic ring at 4 position.

**Acknowledgements** We are grateful to the Department of Science and Technology of Goa 8-213-2013/STE-DIR/Acct/1265 and 8-213-2013/STE-DIR/Acct/135, and UGC- New Delhi F./2015-16/NFO-2015-17-OBC-GOA-37404/(SA-III/Website) for financial support. We would also like to thank Department of Chemistry, Goa University for providing  $^1H$  NMR and  $^{13}C$  NMR data, Department of Chemistry, BITS Pilani Goa campus for XRD data, SAIF Punjab University, Chandigarh for providing NMR and mass spectra. We are also thankful to

Maratha Mandal's NGH Institute of Dental Sciences and Research Center, Belgaum, Karnataka for biological screening facilities.

### Compliance with ethical standards

**Conflict of interest** The authors declare that they have no conflict of interest.

**Publisher's note:** Springer Nature remains neutral with regard to jurisdictional claims in published maps and institutional affiliations.

### References

- Abd El-Karim S, Anwar M, Mohamed N, Nasr T, Elseginy S (2015) Design, synthesis, biological evaluation and molecular docking studies of novel benzofuran–pyrazole derivatives as anticancer agents. *Bioorg Chem* 63:1–12
- Abdel-Aziz M, El-Din A, Abuo-Rahma G, Hassan A (2009) Synthesis of novel pyrazole derivatives and evaluation of their antidepressant and anticonvulsant activities. *Eur J Med Chem* 44:3480–3487
- Ahlstrom M, Ridderstrom M, Zamora I, Luthman K (2007) CYP2C9 structure– metabolism relationships: Optimizing the metabolic stability of COX-2 inhibitors. *J Med Chem* 50:4444–4452
- Ahmed N, Siddiqui Z (2015) Silica molybdenic acid catalysed eco-friendly three component synthesis of functionalised tetrazole derivatives under microwave irradiation in water. *RSC Adv* 5:16707–16717
- Alam M, Alam O, Khan S, Naim M, Islamuddin M, Deora G (2016) Synthesis, anti-inflammatory, analgesic, COX1/2-inhibitory

- activity, and molecular docking studies of hybrid pyrazole analogues. *Drug Des Dev Ther* 10:3529–3543
- Ayati A, Esmaili R, Moghimi S, Bakhshaiesh T, Eslami Z, Majidzadeh K, Safavi M, Emami S, Foroumudi A (2018) Synthesis and biological evaluation of 4-amino-5-cinnamoylthiazoles as chalcone like anticancer agents. *Eur J Med Chem* 145:404–412
- Bole S, Nargund R, Nargund L, Devaraju K, Vedamurthy A, Shruti S (2011) Synthesis and biological evaluation of novel pyrazole derivatives as urease inhibitors. *Der Pharma Chem* 3:73–80
- Desai V, Desai S, Gaonkar SN, Palyekar U, Joshi SD, Dixit SK (2017) Novel quinoxalanyl chalcone hybrid scaffolds as enoyl ACP reductase inhibitors: Synthesis, molecular docking & biological evaluation. *Bioorg Med Chem Lett* 27:2174–2180
- Desai V, Gawandi S (2016) Synthesis of new 2, 4 - dinitro phenyl hydrazone derivatives of chalcones and its biological evaluation. *Indo Am J Pharm Res* 6:4779–4786
- Deng X, Mani N (2008) Regioselective synthesis of 1,3,5-tri- and 1,3,4,5-tetrasubstituted pyrazoles from N-arylhydrazones and nitroolefins. *J Org Chem* 73:2412–2415
- Desai V, Naik S (2013) Use of Solid-Supported Reagents towards Synthesis of 2-Arylbenzoxazole, 3,5-Diarylisoaxazole and 1,3,5-Triarylpyrazole. *Green & Sustain Chem* 3:1–7
- Desai V, Satardekar P, Dhumaskar K, Polo S (2012) Regioselective synthesis of 1,3,5-trisubstituted pyrazoles. *Syn Comm* 42:836–842
- Han Y, Kim K, Choi G, An H, Son D, Kim H, Ha H, Son J, Chung S, Park H, Lee J, Suh Y (2014) Pyrazole-5-carboxamides, novel inhibitors of receptor for advanced glycation end products (RAGE). *Eur J Med Chem* 79:128–142
- Hafez H, El-Gazzar A (2016) Synthesis and biological evaluation of N- pyrazolyl derivatives and pyrazolopyrimidine bearing a biologically active sulfonamide moiety as potential antimicrobial agent. *Molecules* 21:1156–1171
- Holliday D, Speirs V (2011) Choosing the right cell line for breast cancer research. *Breast Cancer Res* 13:215–221
- Keche P, Hatnapure G, Tale R, Rodge A, Kamble V (2012) Synthesis, anti-inflammatory and antimicrobial evaluation of novel 1-acetyl-3,5-diaryl-4,5-dihydro (1H) pyrazole derivatives bearing urea, thiourea and sulfonamide moieties. *Bioorg Med Chem Lett* 22:6611–6615
- Kheder N, Mabkhot Y, Zahian F, Mohamed S (2014) Regioselective synthesis of some pyrazole scaffolds attached to benzothiazole and benzimidazole moieties. *J Chem* 2014:1–5
- Kumar V, Kaur K, Gupta G, Sharma A (2013) Pyrazole containing natural products: synthetic preview and biological significance. *Eur J Med Chem* 69:735–753
- Kumar H, Saini D, Jain S, Jain N (2013) Pyrazole scaffold: a remarkable tool in the development of anticancer agents. *Eur J Med Chem* 70:248–258
- Kumar A, Jain S, Parle M, Jain N, Kumar P (2013) 3-Aryl-1-phenyl-1H-pyrazole derivatives as new multitarget directed ligands for the treatment of Alzheimer's disease, with acetylcholinesterase and monoamine oxidase inhibitory properties. *EXCLI J* 12:1030–1042
- Malvar D, Ferreira R, Castro R, Castro L, Freitas A, Costa E, Florentino I, Mafra J, De Souza G, Vanderlinde F (2014) Antinociceptive, anti-inflammatory and antipyretic effects of 1.5-diphenyl-1H-pyrazole-3-carbohydrazide, a new heterocyclic pyrazole derivative. *Life Sci* 95:81–88
- Mojzych M, Karczmarzyk Z, Wysocki W, Ceruso M, Supuran C, Krystof V, Lipkowska Z, Kalicki P (2015) New approaches to the synthesis of sildenafil analogues and their enzyme inhibitory activity. *Bioorg Med Chem* 23:1421–1429
- Mottamal M, Zheng S, Huang T, Wang G (2015) Histone deacetylase inhibitors in clinical studies as templates for new anticancer agents. *Molecules* 20:3898–3941
- Olender D, Zwawiak J, Zaprutko L (2018) Multidirectional efficacy of biologically active nitro compounds included in medicines. *Pharmaceuticals* 11:54
- Palkar M, Singhai A, Ronad P, Vishwanathswamy P, Boreddy T, Veerapur V, Shaikh M, Rane R, Karpoomath R (2014) Synthesis, pharmacological screening and in silico studies of new class of diclofenac analogues as a promising anti-inflammatory agents. *Bioorg Med Chem* 22:2855–2866
- Penning T, Talley J, Bertenshaw S, Carter J, Collins P, Docter S, Graneto M, Lee L, Malecha J, Miyashiro J, Rogers R, Rogier D, Yu S, Anderson G, Burton E, Cogburn J, Gregory S, Koboldt C, Perkins W, Seibert K, Veenhuizen A, Zhang Y, Isakon P (1997) Synthesis and biological evaluation of the 1,5-diarylpyrazole class of cyclooxygenase-2 inhibitors: Identification of 4-[5-(4-Methylphenyl)-3-(trifluoromethyl)-1H-pyrazol-1-yl]benzenesulfonamide (SC-58635, Celecoxib). *J Med Chem* 40:1347–1365
- Piowar K, Milacic V, Chen D, Yang H, Zhao Y, Chan T, Yan B, Dou Q (2006) The proteasome as a potential target for novel anticancer drugs and chemosensitizers. *Drug Resist Updat* 9:263–273
- Renuka N, Kumar K (2013) Synthesis and biological evaluation of novel formyl-pyrazoles bearing coumarin moiety as potent antimicrobial and antioxidant agents. *Bioorg Med Chem Lett* 23:6406–6409
- Soudy R, H, Etayash H, Bahadorani K, Lavasanifar A, Kaur K (2017) Breast cancer targeting peptide binds Keratin-1 : A new molecular marker for targeted drug delivery to breast cancer. *Mol Pharm* 14:593–604
- Tantawy A, Nasr M, El-Sayed M, Tawfik S (2012) Synthesis and antiviral activity of new 3-methyl-1, 5-diphenyl-1H-pyrazole derivatives. *Med Chem Res* 21:4139–4149
- Topcu Z (2001) DNA topoisomerases as targets for anticancer drugs. *J Clin Pharm Ther* 26:405–416
- Trejo-soto P, Hernandez-campos A, Romo-Mancillar A, Medina-Franco J, Castillo R (2018) In search of AKT Kinase inhibitors as anticancer agents: Structure based design, docking and molecular dynamics studies of 2,4,6-trisubstituted pyridine. *J Biomol Struct Dyn* 36(2):423–442
- Xia Y, Dong Z, Zhao B, Ge X, Meng N, Shin D, Miao J (2007) Synthesis and structure–activity relationships of novel 1-aryl-methyl-3-aryl-1H-pyrazole-5-carbohydrazide derivatives as potential agents against A549 lung cancer cells. *Bioorg Med Chem* 15:6893–6899